Article:

eprints@whiterose.ac.uk
https://eprints.whiterose.ac.uk/

The influence of tool coating on the length of the normal operating region (steady-state wear) for micro end mills

L. Alhadeff[a,*], M. Marshall[b], T. Slatter[b]

[a] *Industrial Doctorate Centre in Machining Science, Advanced Manufacturing Research Centre with Boeing, University of Sheffield, Rotherham, S60 5TZ, UK*
[b] *University of Sheffield, Mappin Building, Mappin St, Sheffield, S1 3JD, UK*

A B S T R A C T

Increasing miniaturisation has significantly increased demand for highly accurate small parts to be machined. Micro milling presents a viable method for series machining parts such as miniature heat exchangers or fuel injectors. Micro end mill tool wear, however, is considerably more difficult to monitor than its macro counterpart, and the tools often fail due to chipping or shaft failure. High tool breakage rates make costs unpredictable and machining times inefficient. Conversely, macro end mill wear is well characterised, and the typical wear curve well understood.

The aim of this work is to elongate the steady state region (SSR) of the wear curve for micro end mills, as this is the practical life of the tool. Coatings can be applied to achieve this, improving wear rates and cutting performance.

This study examines the wear that took place during straight-slot machining with 500 μm micro end mills. This was then compared with observed wear mechanisms on the macro scale. The length of the SSR was used to evaluate the ability of various new coatings to extend the working tool life. The relative predictability in the SSR allows tool paths to be modified to account for changing tool geometry.

The results demonstrate that for micro-mills, the SSR could be elongated, in spite of less predictable wear mechanisms. Overall, this work presents a successful attempt to manipulate the wear curve for micro end mills and highlights the importance of developing an understanding of the wear mechanisms taking place for micro-mills as compared with macro-mills.

1. Introduction

With increased miniaturisation of systems and components, micro milling has emerged as a popular process for manufacturing small components. It is used in industries such as aerospace, medical and dentistry for producing miniature parts such as dental implants and fuel injectors. Furthermore, due to its capability to produce high integrity parts relatively quickly, it has uses in optics and electronics. It also provides a pathway to mass-production through micro-mould manufacturing [1].

Both the medical and aerospace industries make use of materials such as titanium and high-performance superalloys. Nickel-molybdenum alloys, often termed "nickel superalloys" have applications in chemical exhaust processing and similarly corrosive environments for producing heat exchangers or pollution control – such as flue desulfurization systems or fans/fan housings. These are typically difficult-to-machine even on the macro-scale tools, but present further complexity in micro milling as burring and crystal irregularities lead to regular catastrophic fracture of the tools. These high tool fracture rates lead to poor machining efficiency, increased costs and difficulties predicting machining times.

1.1. Typical wear behaviour of milling tools

The typical tool-life wear curve for macro-scale cutting tools is well documented, and a distinct curve can be expected [2,3] as seen in Fig. 1 [4]. Tool wear can be identified as being in one of three zones:

  I. Rapid initial wear
 II. Steady state wear
III. Rapid wear before failure.

In Zone I, rapid wear of the tools is seen as the cutting edge is initially blunted from a very sharp point. During section II a relatively slow, steady increase in wear is seen, referred to as the steady state. Finally, Zone III shows an increase in wear as the tools become severely worn. Fracture of tools occurs in this stage.

This work focusses on the identification of this curve for micro-sized tools (i.e. tools with cutting geometries in the order of micrometers [5]).

The 'tool life criterion' is defined as the point at which the tool begins to wear rapidly [5], at the intersection between phases II and III.

Micro-tool wear monitoring allows process characterisation and establishment of a wear curve that indicates the point at which the tool
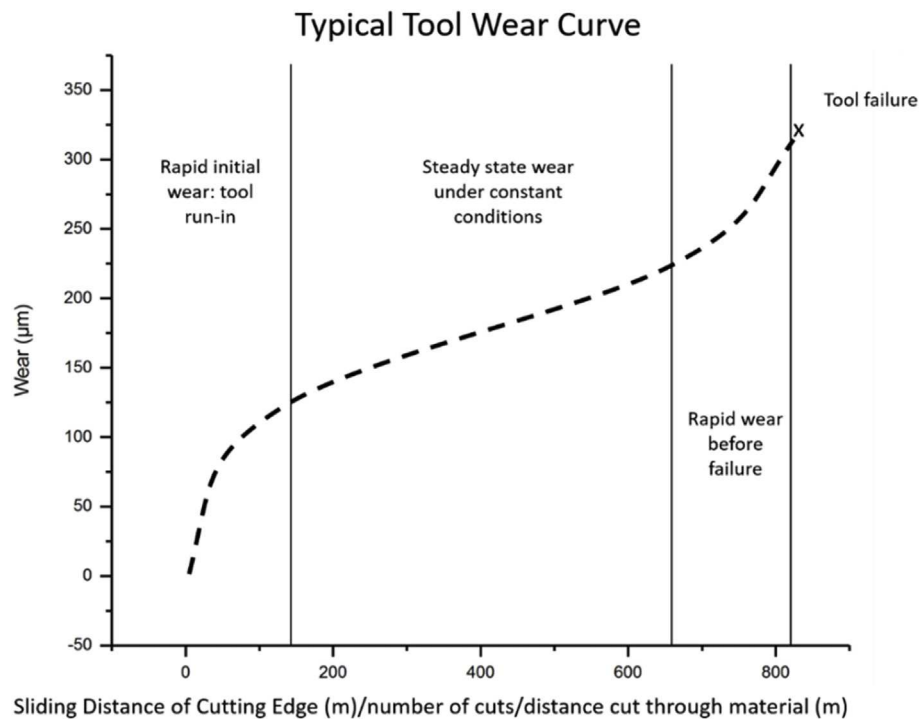

Typical Tool Wear Curve

Fig. 1. The evolution of tool wear of both macro and micro tools, showing I initial run-in, II steady-state wear and III rapid wear before failure.
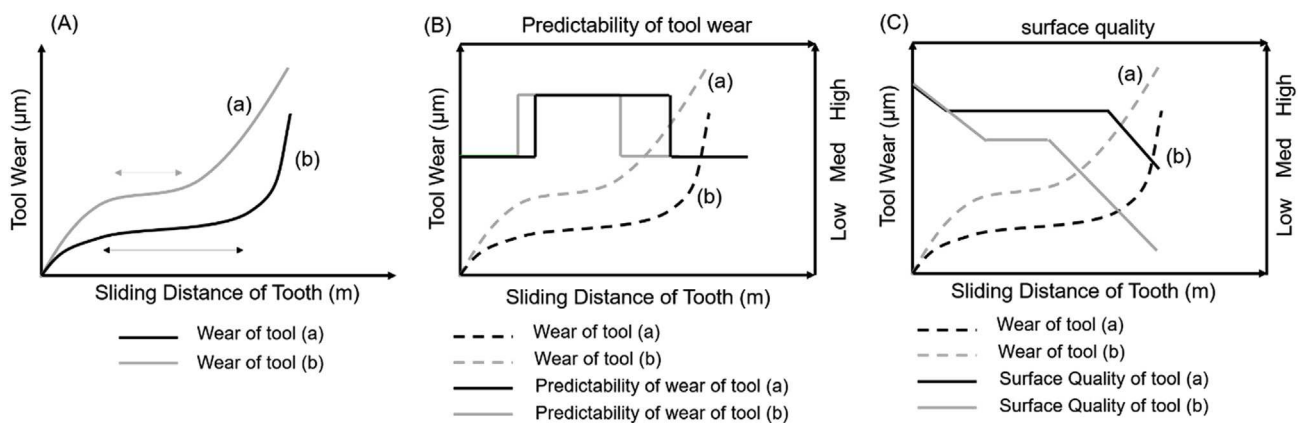

Fig. 2. The three graphs shown give a simplified version of the effects that the region of the wear curve the tool is in has on tool diameter predictions (important for accuracy) and surface quality.

can no longer cut to the required standard [5]. A longer wear curve described in terms of sliding distance is meaningless because it may be that the tool is achieving poor cutting for much of its life. Fig. 2 illustrates this: in Fig. 2a, two tool wear curves of the same overall length are seen, where (b) has a longer SSR. Fig. 2b shows these two curves and a basic value (medium or high) for how easy it is to predict the wear (in terms of reduced diameter) of the tool. Tool (a) shown in grey, is predictable for a much shorter time. Finally, Fig. 2c shows the surface quality for both tools: the tool with the longer steady state results in an overall higher quality part. However, it is challenging to measure tool wear as micro milling cutters generally have poor resistance to fracture [5,6].

1.2. Existing studies into tool wear of micro milling

It is known that the approximation of micro milling as a scaled-down version of conventional milling is flawed: micro milling exhibits different wear and dynamic characteristics. This is known as the size effect [7], and results from relatively large cutting edge radius of tool

compared with depth of cut [8]. Small tool size in relation to workpiece grain size can lead to irregular cutting forces [9] and minor irregularities in tool construction can have catastrophic effects [5].

Furthermore, increased chip clogging compared with macro tools leads to fatigue-related failure and excessive stress-related breakage.

In addition to machining difficulties, there are measurement challenges for very small tools. They cannot easily be measured on-line using a handheld/machine mounted optical microscope due to insufficient magnification or depth-of-field. Thus, tools must be subsequently measured offline using methods such as scanning electron microscopy (SEM). This influences the measurement itself, and can affect run-out.

Despite these issues, a significant body of research into micro tool wear exists [8]. As with macro milling, tool wear is influence by parameters such as cutting velocity and spindle speed [10], feed rate and axial depth of cut [11]. Similarly, there is a consistently positive result between flank wear and cutting forces in end milling (on both macro and micro scales) [12].It follows that reducing cutting forces can reduce the rate of tool wear. One of the methods for this is to apply

coatings to tools, where the mechanism for reduced wear includes altered toughness or reduced frictional forces and therefore reduced heating and wear of tools.

Unlike macro-milling, tool wear measurement for micro tools has traditionally been poorly-defined. There are no unified methods to appraise tool wear [13] and ISO standards cannot be applied to this scale [14]. This has hampered fundamental understanding of the wear processes and makes tool optimisation difficult. Rake face or flank wear has typically been used to provide the best-quality tool wear curves in the context of micro end mills, although often measurement resolution is insufficient [15]. One of the best examples flank wear as a method for producing wear curves is Rajabi et al. [16] who observed a lower overall wear of end mills for TiC based tools with different binders. The practical outcome was improved geometrical accuracy rather than increased tool life (since the tool life criterion occurred at the same point for both tools).

Although geometrical accuracy is essential, the authors focus in this work on extending the working life of the tools, not just absolute wear. Where flank wear is used as a measure of tool wear, it is important to consider the wear on both teeth since even a very small runout has a very significant effect on tooth engagement for micro-tools. Often this is overlooked, and a single tooth is measured to save time [14]. Premature fracture means this type of measurement is inadequate if high fidelity tool wear curves are to be achieved.

As well as flank wear, reduction in diameter is a common metric for measuring micro end mill wear. For full characterisation, this should be considered inadequate as it provides no data on individual teeth and only an overall approximation. Indeed, Oliaei and Karpat investigated the influence of tool wear on machining forces and used both diameter reduction and flank wear as measures of tool wear [17]. The diameter reduction did not allude to a tool wear curve (in fact, it appeared to reduce linearly) whereas the flank wear showed tool wear similar to the traditional tool-life curve described in Fig. 1.

For coarser measurements, reduction in diameter can be measured - for example on-line measurement systems such as light gates, which can provide quick feedback that is useful in measuring geometrical accuracy. Due to the difficulties with measuring micro tools, width of machined slot has been proposed as an indication of tool wear [18]. This did not successfully produce a wear curve and is unreliable as it is highly dependent on run-out of the micro-tool [9]. This was also seen in a previous study by the authors [19]. Outside edge wear is not used to measure wear curves for micro-tools due to significant irregular wear from chips [19].

1.3. The use of coatings in macro and micro milling

The application of different coatings to cutting tools is an established method of increasing tool life on both the macro and micro-scale. Tool life is a critical variable when estimating productivity levels and part accuracy in manufacturing., and that predictable tool wear is desirable since unpredictable tool wear makes prediction of future wear and adjustment of tool paths for improved accuracy impossible.

Increasingly, coatings have been used with varying success at extending micro-tool life [20]. Although coatings can improve tool life, the small scale can lead to a trade-off whereby surface finish is better for uncoated tools due to a smoother tool surface. Often, this is outweighed by the reduced tool-workpiece friction and corresponding lengthening of tool life and reduced burr size seen.

Lower wear rates for coated micro-tools has been attributed to lower friction and hardness of coatings, and the fact that certain coatings suppressed BUE [21], as is seen on the macro-scale [22].

In some studies single-toothed mills are designed to measure wear: for example the effect of PCD coatings on micro end milling of ceramics [23]. Though tool wear curves were seen, in practise single toothed tools are less appropriate for precision or finish micromachining since it affects both productivity [equation (1)] and surface finish [24]. It also

results in increased burr height [25], which is important since burrs are more difficult to remove on micro-parts and should thus be avoided or suppressed where possible [6].

Lin et al. investigated the effect of a PVD applied AlCrN coating for tool inserts in turning [26]. A dramatic increase in performance was seen upon coating the inserts, due not only to increased strength but also due to reduced chemical inertness (important at high temperatures where diffusion wear becomes more likely) and, importantly, reducing friction during machining. This is important since high friction results in high cutting forces, faster tool wear rates, energy losses and high temperatures.

Similarly, Zareena et al. reduced friction at the tool-workpiece interface when machining titanium to a high precision by coating the tools with Perfluoropolyether which in turn resulted in longer tool life and improved surface finish of the tools [27]. They noted that this reduced friction goes some way to reducing the BUE of the tools which is responsible for material pull-out and poor surface finish. Extending beyond coefficient of friction, Neves et al. looked at texturing tools prior to coating to increase coating adhesion and found that the textured tools retained their coating for longer [28], which in turn improved the life of the tools.

It is important to note that improved tool wear is situational: Biermann et al. found that AlCrN and TiAlN, showed improved tool wear but other coatings such as TiN and CrN wore dramatically due to high reactivity between the tools and the workpieces [29]. Due to limited availability of micro-mill coatings, some studies have conducted only very limited comparisons, such as two coatings [13]. This work aims to improve upon this with the used of custom coatings based on those use to cut similar materials on the macro scale. Typically, lower cutting forces are attributed to lower tool-WP friction [30].

$$Q = \frac{a_p a_e v_f}{1000} = \frac{a_p a_e f_z nz}{1000} \Rightarrow Q \propto z \tag{1}$$

Where Q = material removal rate, a_p = axial depth of cut, a_e = radial depth of cut, f_z = feed per tooth, n = spindle speed and z = number of engaged teeth.

As the body of research has increased, the use of coatings on micro mills has focused on specific types of coating, minimising coating thickness and cutting-edge coating technologies. It can be challenging to coat tools in a manner that is appropriate for machining on the micro milling scale. Texturing is difficult, and it is important that coatings applied are thin to minimise edge radius. A coating applied to a micro milling tool will naturally increase the edge radius of the tool which is important when depth of cut is small [20]. Typically, micro-tools studied have been coated using Physical Vapour Deposition (PVD). This is popular with tooling companies due to the lower complexity temperatures required, fine surface finish and low thicknesses achievable which is essential for micro tools [31]. Coating of tools works to lengthen tool life can be extended beyond simply reducing friction at the tool-workpiece interface: Neves et al. looked at texturing tools prior to coating to increase coating adhesion and found that the textured tools retained their coating for longer [28], which in turn improved the life of the tools.

In coating research, AlTiN has seen significant interest. Fox-Rabinovich et al. machined titanium and nickel alloys on the macro scale, and observed that AlTiN coatings combine high plasticity with high impact fatigue fracture resistance, especially important for interrupted cutting, resulting in reduced likelihood of cracks forming compared with TiAlCrN. This significantly improved length of cut over TiAlCrN [32]. Also on the macro-scale, Faga et al. observed that the high COF for AlSiTiN results in a high interface temperature and reduced wear resistance as compared with AlCrN, noting that AlTiN particles removed from the tool contribute to 3rd body abrasion [33].

Multi-layer coatings have also been employed extensively on the macro-tooling scale in milling and turning. Sui et al. developed performed turning tests using a TiAlN/TiAlSiN multilayer coating [34].

Adhesion between the TiAlN and titanium was reported, resulting in BUE, and attributed to a higher wear rate than that seen for TiAlN/TiSiN. It was also seen that the multi-layer reduced spalling over TiSiN alone, due to the protective TiAlN layer.

TiB2 coatings were compared with CBN and PCD inserts by Corduan et al. and less notch wear was observed for the TIB_2 tools. Instead, flank wear and crater on the rake face dominated, due to two-stage wear: coating delamination, and substrate damage. They noted that this is exacerbated where coating-tool adhesion is lower, as in the case of TiB_2.

A limitation with existing research is the focus on overall improvement of cutting tools: surface finish and tool wear at a given time are considered [13], but in spite of conclusions that tool performance is improved, overall tool life is often not investigated and the length of the steady state wear region, a critical factor in tool performance, does not get considered.

The authors propose that to properly develop improved tool design, the length of the steady state wear region should be well characterised and understood, and this has not been adequately carried out in existing research.

In addition, in spite of investigations into coatings on both the micro- and macro-scale, there is little investigation into the relationship between the two. Comparisons between deposition types on inserts give some insight into the expected deposition behaviour of a micro-tool [35] and a number of decent studies into the sliding behaviour of different tool coatings have taken place: Hedenqvist and Olsson comprehensively studied wear mechanisms for TiC-coated carbide and TiN-coated steel [36]. However, this fundamental study provides no insight into the different behaviour of these materials under workshop conditions. Furthermore, the use of a different substrate presents an extra variable. A study that compared PVD ZrN coated carbide in both sliding tests did observe wear mechanisms in both turning and in a sliding wear test, but links between the two physical environments were made and the dominant wear mechanisms not explained [37]. Similarly, the work took place using turning, on the macro scale, which tells us little about micro-milling [38].

This work relates the wear behaviours seen on pin-on disc tests for coatings used on micro-tools, to those seen during machining. As a result, comparisons can be made between wear mechanisms on the macro and micro-milling scales. This is novel on two counts:

1. It is acknowledged that wear behaviour differs on the micro-scale, but this often poorly explained. There is also much more limited research onto micro-mill coatings.
2. Similarities seen between the micro-and macro-scale allow technologies from macro-milling to be adapted to a smaller scale.

1.4. Expected wear

Typically abrasive wear often dominates the wear of macro-tools, resulting in a defined tool wear curve (Fig. 1) [4]. Adhesive wear, resulting in a Built-Up-Edge (BUE) is also common. High temperatures at the tool-chip interface can lead to plastic deformation and cracking, while crater wear and edge chipping are also seen.

In a preliminary study by the authors, uncoated 0.5 mm tools were used to machine a Nickel–Molybdenum (NiMo) alloy, brass and titanium. Qualitative observations of this revealed that abrasive wear was the dominant method of failure for the tools (Fig. 3). For these tools, wear rate was more constant and relatively more predictable than for the other micro-milling tools.

1.5. Motivations for current work

The underlying aim of the current work is to increase the life of the tools being used. In doing so, it is intended that machining processes will be more efficient due to fewer tool changes, and that accuracy for micro milling operations can be more tightly controlled. To achieve the
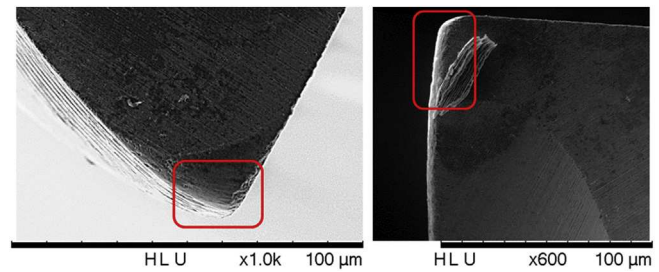

Fig. 3. An uncoated tool is imaged using SEM. Both images highlight areas where abrasive wear dominated.

latter, the time (or machining distance) that the tool spends in steady state wear (identified as Phase II in Fig. 1) must be maximised.

The novelty of this work is derives from the following aims:

Aim 1. To extend the length of the steady state wear region (SSR) using coatings not previously applied to micro-mills, since this region represents the operating region where tool wear is predictable (and hence can be adjusted for),

Aim 2. To reduce the length of the tool run-in time, allowing the SSR to be reached more quickly and so reducing the nonlinear region of wear.

Three materials were chosen for this work: brass, for its easy machinability and application in producing miniature gears which do not need lubrication [39], titanium grade 2 for its applicability in the medical and dental industries [40–42] and NiMo as it is difficult-to-cut due to high temperatures, adhesive and diffusion wear, and the formation of BUE [43]. NiMo is difficult-to-cut due to high temperatures, adhesive and diffusion wear, and the formation of a BUE [43].

2. Methodology

To evaluate the length of SSR of the tools the relative performance of generic AlTiN coatings with custom coatings was examined. Experiments were designed to observe tool wear regularly across the life of the tool. Two possible outcomes were expected:

Towards aim 1. Observation of the improvement in this region over the original coating would take place (thus validating the assertion that tool design can be used to extend this region and fulfilling the first aim of this work). Alternatively, this region would remain the same and tribological observations could be used to inform further design.

Towards aim 2. Reduction of length of run-in. The coatings were designed with the intention to achieve this.

It should be noted that there is some degree of trial and-error regarding this. It is intended that the understanding of wear mechanisms developed through this work will help reduce run-in time.

Tools of 0.5 mm diameter consisting of fine-grained tungsten carbide coated with Kyocera proprietary coatings were used to machine three materials: Brass (CuZn37); Titanium (Grade II); and NiMo (specifically, Hastelloy C-276).

The materials were machined using tool coatings depicted in Table 1. Cutting parameters (Table 3) remained the same for each material.

All tools were coated using HiPIMS (High Power Impulse Magnetron Sputter) which results in a smooth finish, to minimise the effect that varied coating geometries have on the micro-scale. The material properties are given in Table 2.

The trials took place on a KERN Evo micro milling machine with a maximum spindle speed of 50,000 RPM. Straight slots of 25 mm in

Table 1
Coatings used for each material and measurement intervals.

Workpiece	Coating	Parameter Set	Sliding distance between observation (m)
Brass	**AlTiN**	1	0.0125
Brass	**TiB$_2$**	1	0.0125
Titanium	**AlTiN**	2	56
Titanium	**TiAlN/TiSiN**	2	28
NiMo	**AlTiN**	3	26
NiMo	**AlTiCrN**	3	24

Table 2
Mechanical properties of the coatings tested as quoted by the manufacturer.

Coating	TiAlN	AlTiN	TiB2	TiAlN/ TiSiN	AlTiCrN
Microhardness (GPa)	28	38	39	37	34
Friction Coefficient (Fretting, steel ball)	0.3	0.7	0.9	0.6–0.9	0.24
Typical thickness (μm)	1–4	2–4	2	1.5–3	3
Maximum working temperature (^{0}C)	700	900	900	1100	1100

Table 3
Machining parameters used to machine the three materials tested. These were consistent across different coatings.

	Brass (1)	Titanium (2)	NiMo (3)
Spindle speed (rpm)	50000	25205	6786
Feed (m/min)	479	69	11
F_z (mm)	0.00479	0.00136	0.00080
Radial depth of cut (mm)	0.5	0.5	0.5
Axial depth of cut (mm)	0.2	0.2	0.2
Sliding distance per 25 mm length (m)	4.016	14.06	23.75

length were milled to a depth of 0.2 mm. The workpiece and tool were flooded continuously throughout the cutting process using synthetic Hocut 768.

The tools were measured both prior to testing and during testing using a standardised methodology [19] as indicated in Section 1.2. During machining, the tools were then removed at pre-determined intervals for measurement using an SEM using both secondary electrons (SE) and the back-scattered electrons (BSE) to allow optimal opportunity to recognise wear features. The tools are imaged in two orientations: side-on, and face on as shown in Fig. 4.

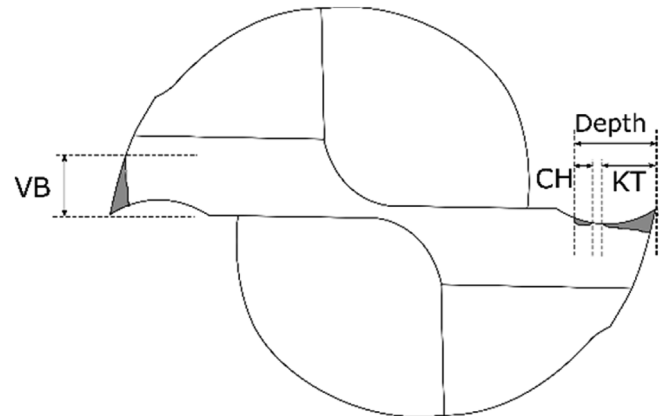Three types of wear were measured: flank wear, denoted VB; rake

Fig. 5. Flank wear is denoted VB, while rake face wear is denoted KT.

face wear, denoted KT., and outside edge wear, denoted OE (Fig. 7, Fig. 5). The measurement process was as follows:

1. Tools were washed in acetone, and then air-dried to remove swarf and dust before:
   a. Imaging in a SEM using both scattered and backscattered electrons
   b. Analysis in image measurement software to determine the type and extent of wear seen.
2. Tools were then replaced and steps 1–2 repeated.

Catastrophic failure was recorded in the cases of the loss of one or both teeth (as seen in Fig. 6) All wear measurements are expressed in terms of μm.

Use of sliding distance allows a more consistent metric to measure tool wear against than cutting distance or cutting time, as the amount of work carried out on the tool depends on spindle speed and feed rate.
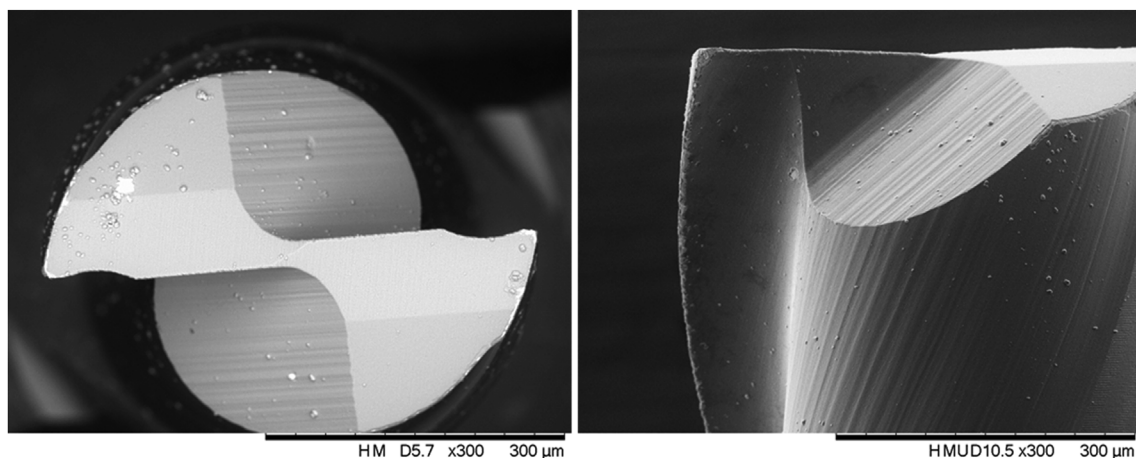

Fig. 4. The tools were measured in the two orientations shown, with rake face and flank wear considered from the end-on perspective (Left), and chipping considered from the side-on perspective (Right).
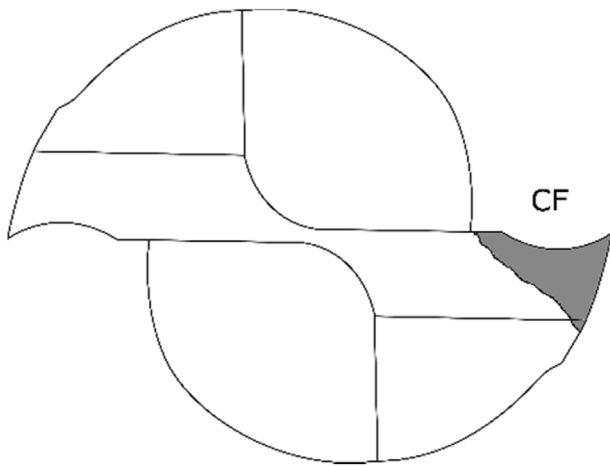
Fig. 6. If one or both teeth were lost, catastrophic failure (CF) was indicated.

This was calculated using Equation (2).

$$x_{comp} = \pi D_{cap} c_{comp} + \sum_1^{c_{inc}} x_i \tag{2}$$

Where c_{inc} is number of complete circles, calculated by

$$c_{inc} = \left(\frac{D_{cap}}{s} \right) - D_{cap} mod1$$

c_{comp} is the number of complete circles, calculated by $n_{rev} - c_{inc}$, D_{cap} is engaged tool diameter, n_{rev} is the number of the revolutions of the tool and $\sum_1^{c_{inc}} x_i$ is the sum of the sliding distances for all the incomplete circles.

The value of x_{comp} was calculated using a Matlab program which established $\sum_1^{c_{inc}} x_i$. (Sliding distance per 25 mm is given in Table 3).

To further investigate wear mechanisms, coated discs were tested using a pin on disc machine (Bruker UMT), Coatings of the same thickness as those applied to the micro-tools tested using reciprocating-sliding pin-on-flat tests (Fig. 8). A vertical load applied to the surface acting along the axis of the pin simulated the wear mechanisms experienced by the tools. An 8 mm diameter AISI 52100 steel ball was used to apply contact pressures to simulate those experienced by the tools during machining. A reciprocating motion with a speed of 40 mm/s was used.

3. Results

In micro-milling, challenges in measuring tools result in relatively large measurement errors. This is due to the difficulties in identifying
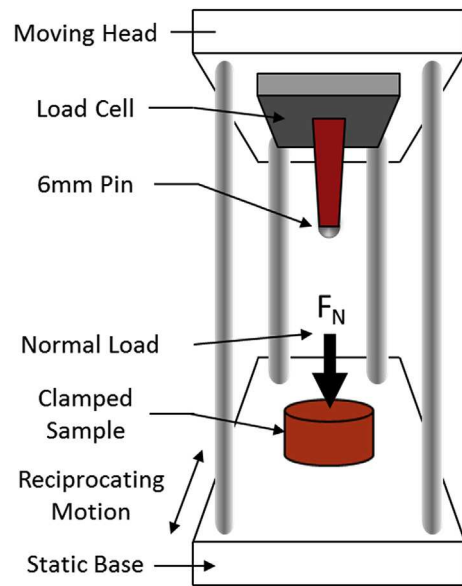

Fig. 8. Schematic of the UMT used to carry out pin-on-disc testing of samples.

exactly where wear has taken place, even using high-quality images. Wear is measured here using similar metrics as those used for macro-milling, but here the wear is much greater relative to the overall size of the tool. Errors are considered in Section 3.1 and are displayed as error bars on the graphs.

In this study, information is only taken for teeth which did not experience catastrophic failure to circumnavigate this issue. Tool wear for both flank and rake face are provided for NiMo alloy and titanium. Experiments on brass took place earlier, alongside the development of a standardised tool wear measurement protocol.

3.1. Sources of error

Both teeth for each tool were marked separately, and wear measured for each tooth. For each tooth, two images were taken, one using secondary electrons (SE) and the other using back-scattered electrons (BSE). The wear measured for both teeth was then averaged to give a mean tooth wear for the tool (Equation (3)), and errors were calculated to be standard deviation for all images, and then propagated (Equation (4)).

$$T_\mu = \frac{T_{1,SE} + T_{1,BSE} + T_{1,SE} + T_{1,BSE}}{4} \tag{3}$$

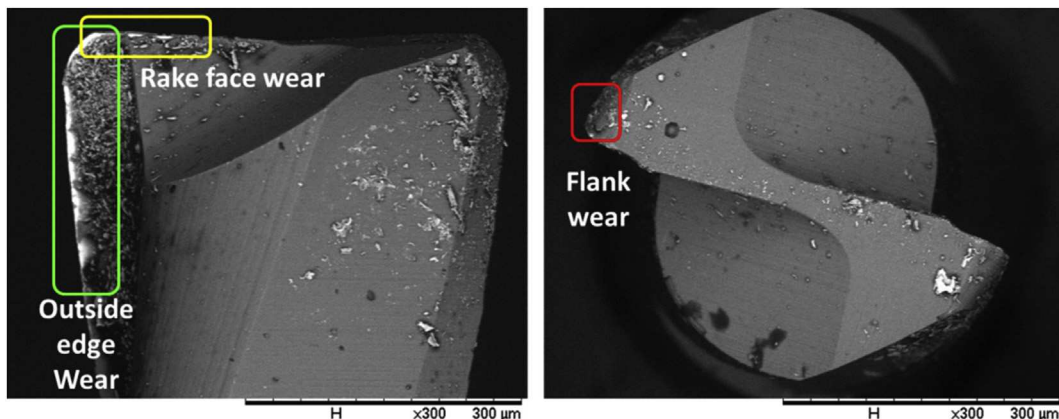Where T_μ is the mean tooth wear for one tool, and $T_{n,xE}$ denotes tooth

Fig. 7. The three types of wear described, rake face, flank and outside edge, were measured as shown.
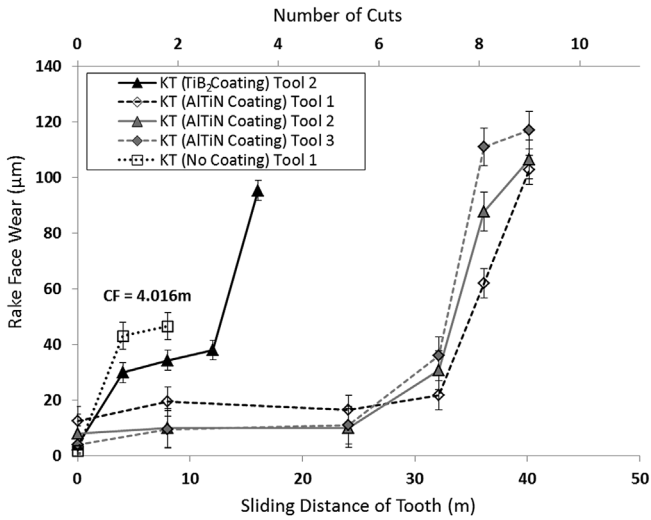
Fig. 9. Tool wear plotted for tools used to machine brass with different coatings (TiB$_2$ and AlTiN). CF indicates catastrophic failure of the tool.

Fig. 10. Rake face wear for tools used to machine titanium grade 2. TH coating is TiAlN/TiSiN.

number, n, and image type xE.

This gives errors of

$$\Delta T_1 = \frac{|T_{1,SE} - T_{1,BSE}|}{2}$$

$$\Delta T_2 = \frac{|T_{2,SE} - T_{2,BSE}|}{2}$$

and

$$\Delta T_\mu = T_\mu \sqrt{(\Delta T_1)^2 + (\Delta T_2)^2} \qquad (4)$$

3.2. Comparison between TiB$_2$ tools and an AlTiN coating for CuZn38 brass

Fig. 9 shows a comparison between the TiB$_2$ tools used to machine brass, and the tools which were coated with AlTiN. The steady state portion of the graph is over twice the length for AlTiN. The uncoated tool used for comparison fractured early in the machining, confirming its unsuitability.

3.3. Comparison between AlTiN coated tools and TiAlN/TiSiN for cutting titanium grade 2

For face wear, the tool wear curves for the AlTiN and TiAlN/TiSiN coatings used to machine titanium grade 2 have a similar length SSR for both types of coating (Fig. 10). This occurs at a lower wear level for the TiAlN/TiSiN coating.

For flank wear, on the other hand, the TiAlN/TiSiN coating does not enter stage III of wear during the measurement period, and a long SSR is seen. This region also takes place at a slightly lower degree of wear than for the AlTiN coating (Fig. 11).

3.4. Comparison between AlTiN coated tools and AlTiCrN for cutting NiMo

The AlTiCrN coated tools showed a decreased length of steady state wear and stage III wear for the rake face of the tools, and indeed for the flank of the tools (Fig. 12). The original AlTiN coated tools had both a longer and more clearly-defined SSR (see Fig. 13).

4. Discussion

4.1. Relationship between SSR and RIP as a measure of performance

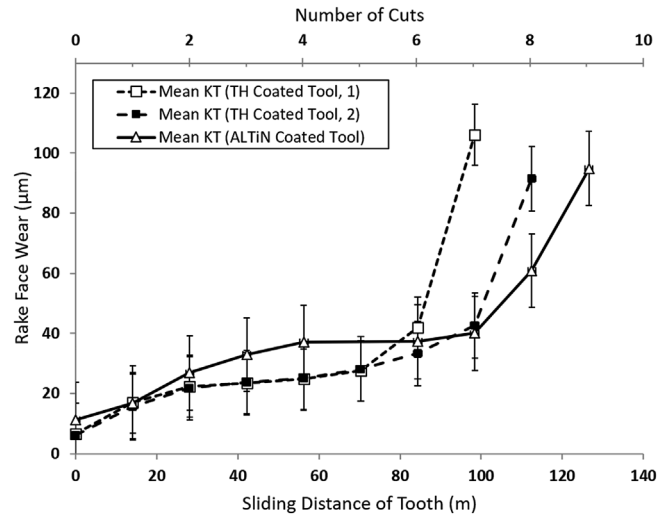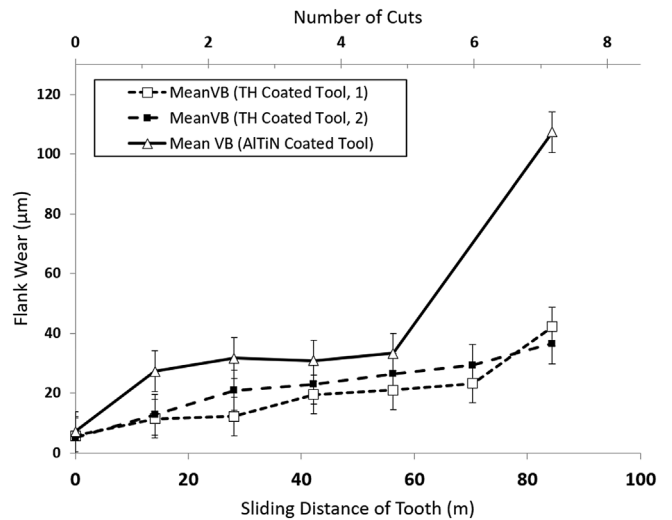The relative performance of coatings can be compared by

Fig. 11. Flank wear for tools used to machine titanium grade 2. TH coating is TiAlN/TiSiN.
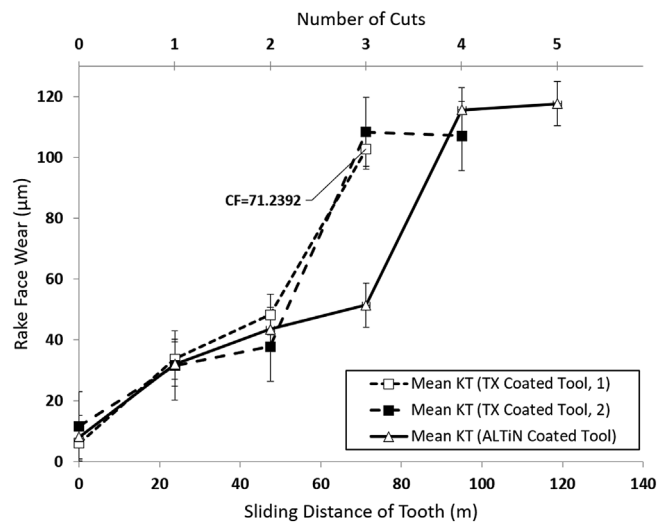

Fig. 12. Rake face wear for tools used to machine NiMo. TX coating is AlTiCrN.
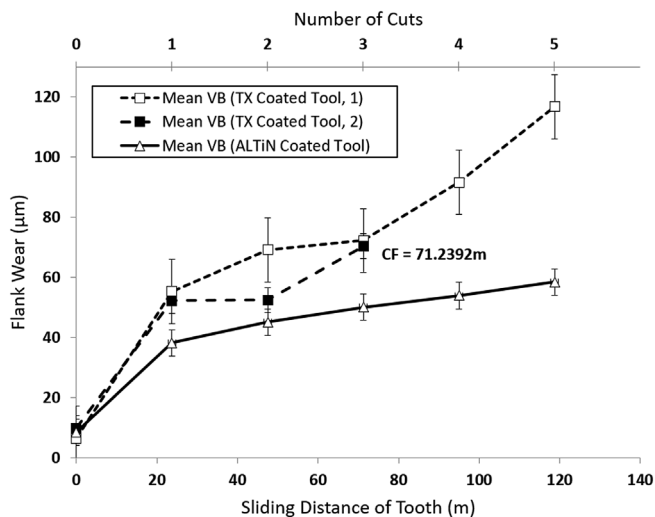
Fig. 13. Flank wear for tools used to machine NiMo. TX coating is AlTiCrN.
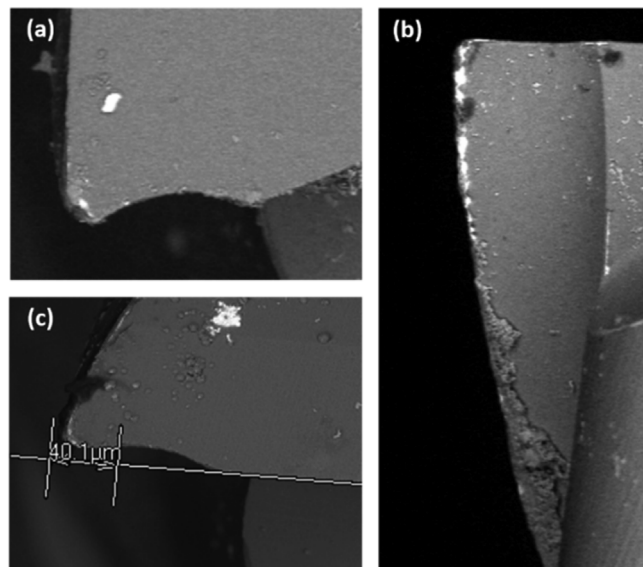

Fig. 14. Three images of teeth: (a) and (b) are the front-on and side-on views for TH-coated tool, while (c) is the front-on view for an AlTiN coated tool.

comparing the length of the run-in periods (RIP) of the tools to their steady-state wear region (SSR). RIP is used since it represents an unpredictable period of machining. Rake face wear was used as complete datasets were available for all three types of material.

The criterion for higher tool performance is to have a proportionally higher SSR when compared with other areas of the wear curve. For the tools used to cut brass, the SSR:RIP ratio was much higher for AlTiN, and thus AlTiN performed better. Coating performance for each material is discussed with respect to wear mechanisms seen.

For each material, the SSR was longer where overall tool life and performance was better, verifying that length of steady state region is indeed a useful measure of tool life and indicator of performance. This was especially clear in the cases of brass and NiMo, where AlTiN and TiAlN/TiSiN increased the SSR by factors of 4.3 and 2.6 respectively. For titanium and NiMo, when the tools performed better the SSR was longer and occurred at a lower level of absolute wear (Section 3.2).

Comparisons between the AlTiN coating used to machine all three materials and the relative rake face wear verify that where tool performance was better, SSR was relatively longer in the context of the whole curve. Thus, in each case, SSR proves to be a good metric for predicting tool life.

4.2. Coating performance and wear for brass

Table 4 and the graph in Fig. 9 revealed:

(1) A dramatic lengthening of the steady state region of the tool wear curve for AlTiN coated tools.
(2) That the steady state region of wear for the TiB$_2$ tools occurred at a higher level of wear than that for the coated tools.

Observation (2) is noted in literature [16], but a longer SSR presents a significant result as it indicates a longer tool life. For best

Table 4
Calculated ratio of SSR to RIP for milling tools.

Coating	Workpiece	Face of Tool	Mean RIP (m)	Mean SSR (m)	SSR: RIP
AlTiN	Brass	Rake	2	26	13
TiB$_2$	Brass	Rake	4	6	1.5
AlTiN	Titanium	Rake	56	42	0.75
TiAlN/TiSiN	Titanium	Rake	28	49	1.75
AlTiN	NiMo	Rake	26	52	2
AlTiCrN	NiMo	Rake	24	24	1
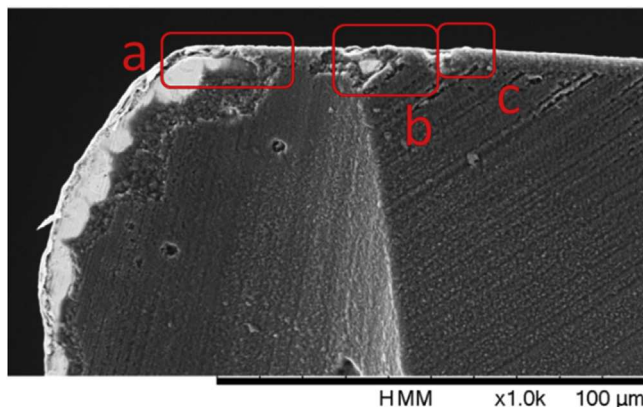
Fig. 15. Examples of micro-chipping to the coating, exposing the tool underneath (a) shows the cross section of the tool on coating, where coating has been removed. (b) shows a smaller chip where the substrate is still fully exposed, and (c) shows a chip of partially removed coating.

performance, the SSR should ideally occur when the tool is less worn.

Over their life, the AlTiN tools exhibit some adhesion to workpiece but primarily abrasion across the edges of the teeth (Fig. 14), with exposure of tool material underneath. The workpiece adheres more to the TiB$_2$ tools, and more plastic deformation is seen. Brass exhibits high adhesion in machining [44], which contributes to the adhesive wear observed (see Fig. 15).

On a macro-scale, TiB$_2$ is a brittle material [45] that adheres to the workpiece during machining. This may explain why, in comparison to the AlTiN, large parts of the coating have fractured earlier in the wear. Abrasion occurs later in the tool wear, after parts of the coating have been removed.

This is seen in both macro and micro-tools [37], but the issue is exacerbated on the micro-scale due to difficulty in flushing small abrasive particles on a smaller scale [46], and smaller edge radii which expedite mechanical failure.

4.3. Coating performance and wear for titanium

The TiAlN/TiSiN demonstrated a better SSR:RIP than the AlTiN (Table 4) and a lower overall level of wear (Fig. 10 – Rake face wear for
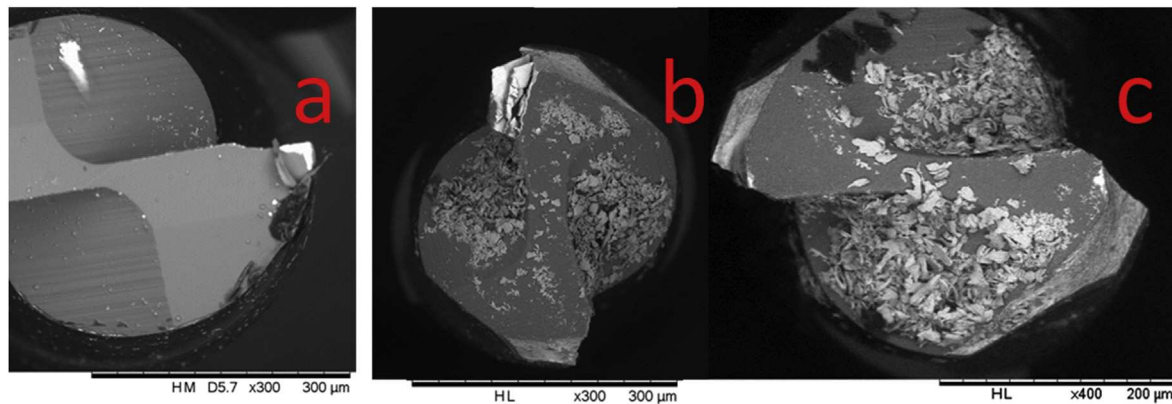
Fig. 16. (a) shows peeling of the coating, (b) shows severe cracking to one of the teeth after a cut. 100 mm later, the entire tooth has fractured (c), thus the failure mode here was cracking.

tools used to machine titanium grade 2. TH coating is TiAlN/TiSiN.for the TiAlN/TiSiN coating. SEM images of both AlTiN and TiAlN/TiSiN coated tools (Fig. 16) taken show removal of coating.

Some chip adhesion and chipping of the rake face of the TiAlN/TiSiN tool is seen (Fig. 16a). Comparatively, wear of the rake face for the AlTiN tool seems smoother and less irregular (Fig. 16c). This suggests that there is some interaction between the TiAlN/TiSiN coating [27] and the titanium, which is known to be chemically active [27,47]. This results in increased wear rates on the rake face, and exposure of the rake face to excess forces as a BUE forms. Thus, even if the TiAlN/TiSiN coating is theoretically more resistant to wear than the AlTiN coating, it wears quickly. Furthermore, material has not built up on the flank, which possibly explains the longer SSR for the TiAlN/TiSiN tools.

Fig. 16b shows the side-on view of the TiAlN/TiSiN tool, where material has adhered to the rake face. Such interaction is often seen between carbide and coated carbide tools; and workpiece materials, in both macro- and micro milling: for example, Nouri and Ginting observed both adhesion wear and diffusion wear when machining Ti–6242S, observing that both the rake face and flank experienced diffusion wear [48].

Similar wear mechanisms are seen for macro-tool coatings containing Ti, Al and Si to those observed here [30]. The higher rate of wear for smaller tools is influenced by a very small tool-chip interface which results in higher stresses for micro tools [5], and the poor heat conductivity of titanium [30]. Chipping is seen on both scales due to a high chemical reactivity with titanium which leads to welding. For the TiAlN/TiSiN more adhesion was seen due to the addition of silicone, which has been seen on both the macro and micro-scale for milling and turning [49]. However, the silicone increases wear resistance by hardening the material and homogenising grain structure, which results in better tool performance in spite of increased adhesion [50].

4.4. Coating performance and wear for NiMo

The AlTiN performed better than the AlTiCrN coating (Table 4) in terms of SSR:RIP and the absolute wear of both coatings during the SRR for each tool was similar (Fig. 12). The length (and consistency of gradient) of the SSR of the tool wear curves is greater for both rake face and flank wear for the AlTiN tool than the AlTiCrN tool. Thus the rate of wear can be much better predicted for AlTiN, and end workpiece geometry more easily controlled. For macro tools this was similarly noted by Fox-Rabinovich et al. This was attributed to the high plasticity and impact fatigue resistance which reduces tool fracture [32].

A significant BUE and some removal of chips or areas of coating is seen for the AlTiN. However, the AlTiCrN coating exhibits primarily removed areas of coating – fatigue due to adhesion – which appears to result in rapid abrasive wear. Abrasive wear is likely to be caused by

areas of removed coating acting as abrasive particles.

A similar run-in gradient was seen for both the AlTiCrN and the AlTiN coated tools. Both of these tools have a low COF: however, the adhesive properties of NiMo result in significant wear during run-in compared to other materials.

Carbide particles in NiMo can contribute to abrasive wear for macro-scale cutting tools [39], and indeed this was seen to some extent during machining. Work carried out by Ucun et al. and 4 mm end mills supports this result [21]. Ucun used Inconel; compositionally similar to NiMo thus comparison is reasonable. The macro-tools also showed significantly more built-up material for the CrN-containing coating, due to an affinity between the coating material and workpiece. More corner-chipping and chipping was seen for the CrN tools, while the AlTiN demonstrated peeling of coating.

SEM micrographs of the micro-tools revealed very similar wear mechanisms to the discs, suggesting that the tribological behaviour of the tools is dictated primarily by the coating and workpiece, while the increased wear on micro-tools over macro tools reflects the geometrical issues faced.

Interestingly, the AlTiN tools exhibited increased wear on the macro-scale, this is because the affinity between the AlTiCrN coating and NiMo results in increased adhesion leading to chipping by fatigue. Whereas on the macro-scale this contributes to wear over time, on the micro scale area of coating removed is very large compared to the overall size of the tool, after which catastrophic failure occurs (Fig. 18) through severe abrasion and chemical wear.

Similarly, micro-tools suffer from catastrophic failure due to edge chipping [17] earlier than macro tools, grain removal represents a significantly larger area of the tool. Thus, tribologically, there are significant similarities, but mechanically wear mechanisms are influenced by size.

These effects, and the impact from interrupted cutting, are exacerbated by the irregularity of the boundaries between grains which are large compare with the cutting tooth. Overall, wear is similar on both macro-and micro scales, but relatively larger chunks of coating material on the micro-scale contribute to more irregular wear.

4.5. Differences between wear mechanisms seen in micro and macro

For each coating tested the results for the micro-tools have been compared to macro tests with good agreement, seeing evidence of abrasion, adhesion, BUE and plastic deformation. However, in many cases the nature of the tool geometry on the micro scale appears to have modified or accelerated wear mechanisms, therefore, to further explore these points, pin-on-disc testing was undertaken. The coatings were tested using a reciprocating-sliding pin-on-flat tests represented the actual thicknesses of coatings applied to the micro-tools. A vertical load
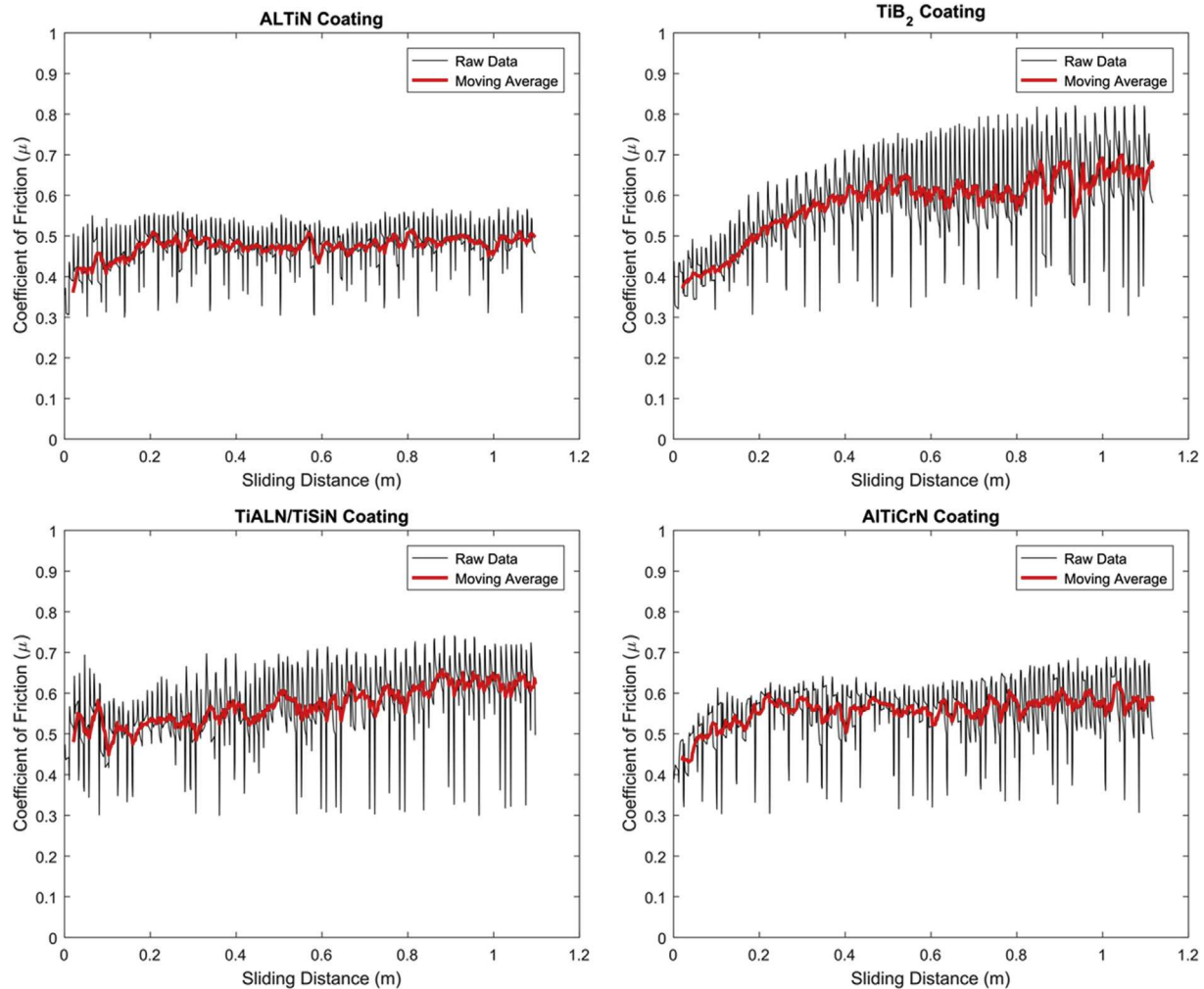
Fig. 17. Friction coefficient measured during UMT tests is given for the four coatings over 1 m of sliding distance.

applied to the surface acting along the axis of the pin simulated the wear mechanisms experienced by the tools. An 8 mm diameter AISI 52100 steel ball was used to apply contact pressures similar to those seen in the machining to flat coated discs, with a reciprocating motion at a speed of 40 mm/s.

However, the disc removed the geometrical effects of the tools. This allowed a comparison between the micro-and macro behaviour of the coatings to be considered, since literature regarding coatings is typically very specific to workpiece and material. Significant conclusions have been drawn from sliding tests which support mechanisms seen on the micro-scale and highlight relationships between the micro and macro scale. Friction data for each material can be seen in Observations for AlTiN wear mechanisms.

4.5.1. Observations for AlTiN wear mechanisms

For AlTiN, observation of the COF (Fig. 17) in sliding tests showed that over the first 0.2 m the COF has increased by approximately 0.1. This indicates that some adhesion is taking place, rather than simply abrasion, supporting the data seen in the machining trial. Optical images of the disc revealed mostly adhesive wear (Fig. 18), where coating removal takes place by fatigue due to adhesion. As in machining tests, abrasion was seen later when a third body – flakes of the coating – was introduced (Fig. 18). Delamination and detachment of AlTiN coating by brittle failure, which lead to third body abrasion was also observed by Aihuia et al. during pin-on-disc tests [38]. This is exacerbated by the sharp tool geometries which cause stresses on the coating at the cutting edge [44].

Comparing this to the micro-milling trial, SEM images of the tools show first adhesive wear, and later abrasive wear. Faga et al. also saw abrasive wear from 3rd body abrasion, and here some grain detachment is seen after 10 test runs which contributes to this [33]. AlTiN tools showed abrasive wear after a much shorter time than the discs, reflecting the geometrical weaknesses of the sharp teeth, and impact wear was also seen based on the interrupted cuts.

4.5.2. Observations for TiB₂ wear mechanisms

For TiB_2, the COF is increased from 0.4 to 0.65 over 1 m, as adhesive contact area increased. Intense adhesion explains occurrence of the SSR for the TiB_2 tools at a higher absolute level of wear. This has also been seen in macro-milling operations [51].

As with the AlTiN, TiB_2 tools used to machine brass exhibited, during sliding tests, both plastic deformation and a BUE early in the wear and later abrasion and removal of coating (Fig. 21). There was also adhesion of chips to the tool which contributed to adhesive wear. In a machining context, TiB_2 has both a higher working temperature and a higher coefficient of friction with steel to AlTiN, which results in comparatively higher temperatures and plastic deformation.

Coating was removed early for the TiB2 tools. After only two measurements significant loss can be seen (Fig. 19). This suggests relatively poor adhesion of coating to tool, as suggested by Corduan et al. Craters and notching are then seen (Fig. 20), with substrate exposed to chemical and adhesive wear, and tools fail quickly [45].
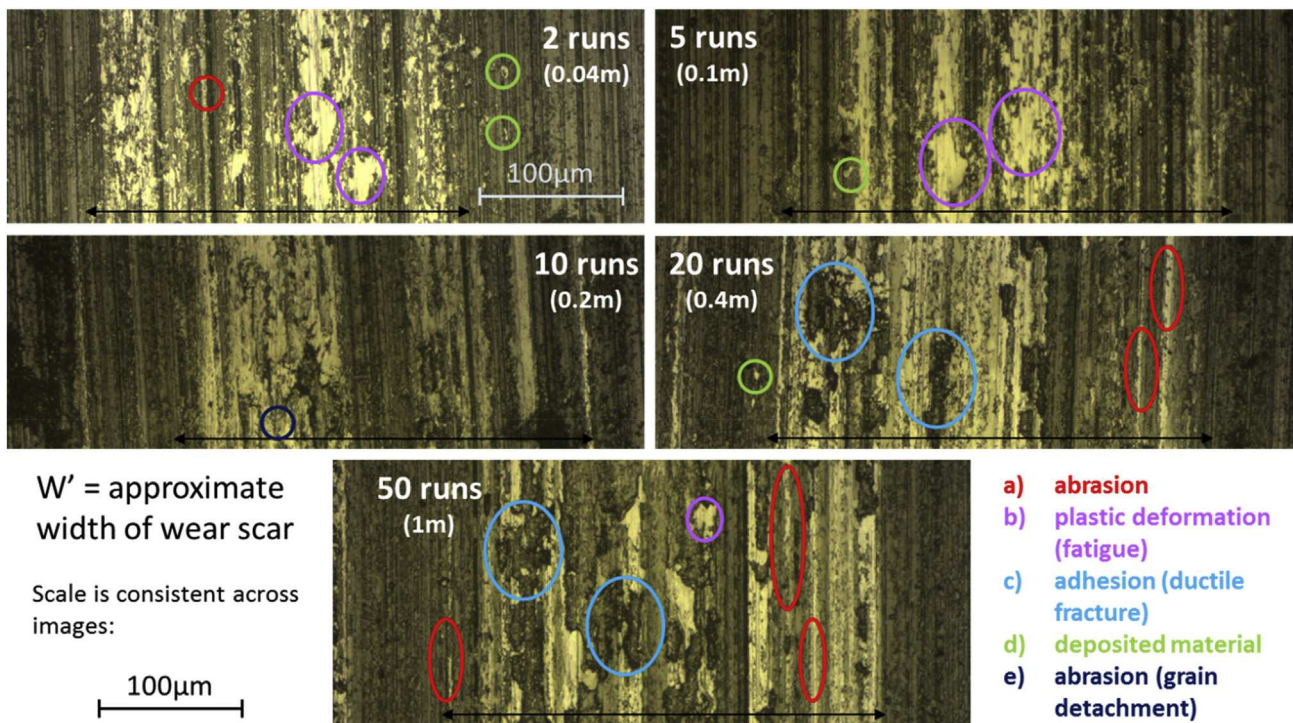
Fig. 18. Wear is observed optically after 2, 5, 10, 20 and 50 runs. Some types of wear observed are highlighted here.
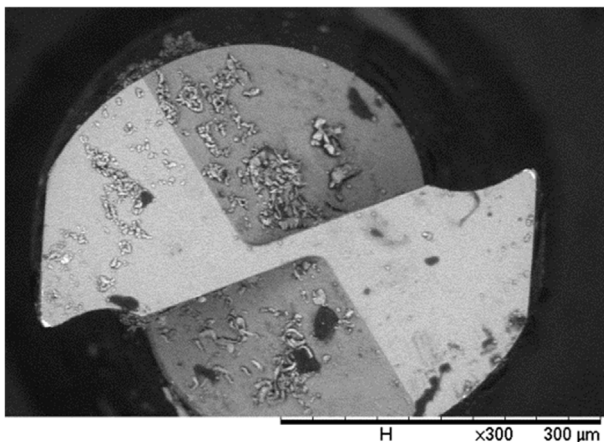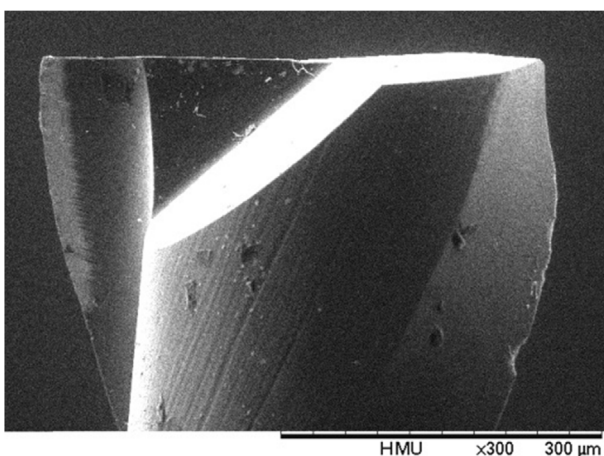

Fig. 19. Tool Wear after only two cuts.

Fig. 20. Loss of coating has resulted in notching.

4.5.3. Observations for TiAlN/TiSiN wear mechanisms

COF between TiAlN/TiSiN and disc was initially higher than for AlTiN, at 0.5. However, it increased less over the wear distance. For TiAlN/TiSiN coating abrasive and adhesive wear were seen, leading to coating fatigue and then pitting towards the later stages of coating wear (Fig. 17). A cross-section of the coating layer was visible. After coating removal, the carbide is then vulnerable to rapid abrasive and chemical wear due to chemical affinity between the tools, exacerbated by high temperatures. This is supported by the conclusions of Faga et al. [33], who attributed these high temperatures to a high COF. It is reasonable to compare in spite of the fact that Faga et al. investigated macro tools since the disc testpieces do not have micro geometry and the coatings are of similar thickness. Coating removal for the disc was influenced only by fatigue due to adhesion; with abrasion occurring later as for AlTiN (Fig. 22). Siu et al. saw this and also spalling, which can be seen in the Fig. 22 and contributes to abrasive wear [34].

4.5.4. Observations for AlTiCrN wear mechanisms

Less ductile fracture was seen than for AlTiCrN than the AlTiN coatings, in spite of higher plastic deformation: thus the tools wore less dramatically. A smoother surface caused by abrasion would likely reduce the COF which suggests that some adhesion is taking place, verified by optical images taken. This supports the data seen in the machining trial.

Finally, COF for AlTiCrN increased linearly for the first 0.2 m, before plateauing. Wear evolved primarily by adhesive mechanisms. Early on, the primary effect seen was some plastic deformation which increased linearly. After 0.2 m, the addition of both ductile fracture and surface fatigue were seen, increasing over sliding distance (Fig. 23).

Deep pitting, corresponding to tool chipping in a machining context, was later seen and more plastic deformation than for AlTiN coating. When tools were used to machine, the primary issue with adhesion was the formation of a BUE which, due to the geometry of the tool, can easily cause catastrophic material removal from the tool. This leads to notching which has been observed experimentally both in this and other studies [21].

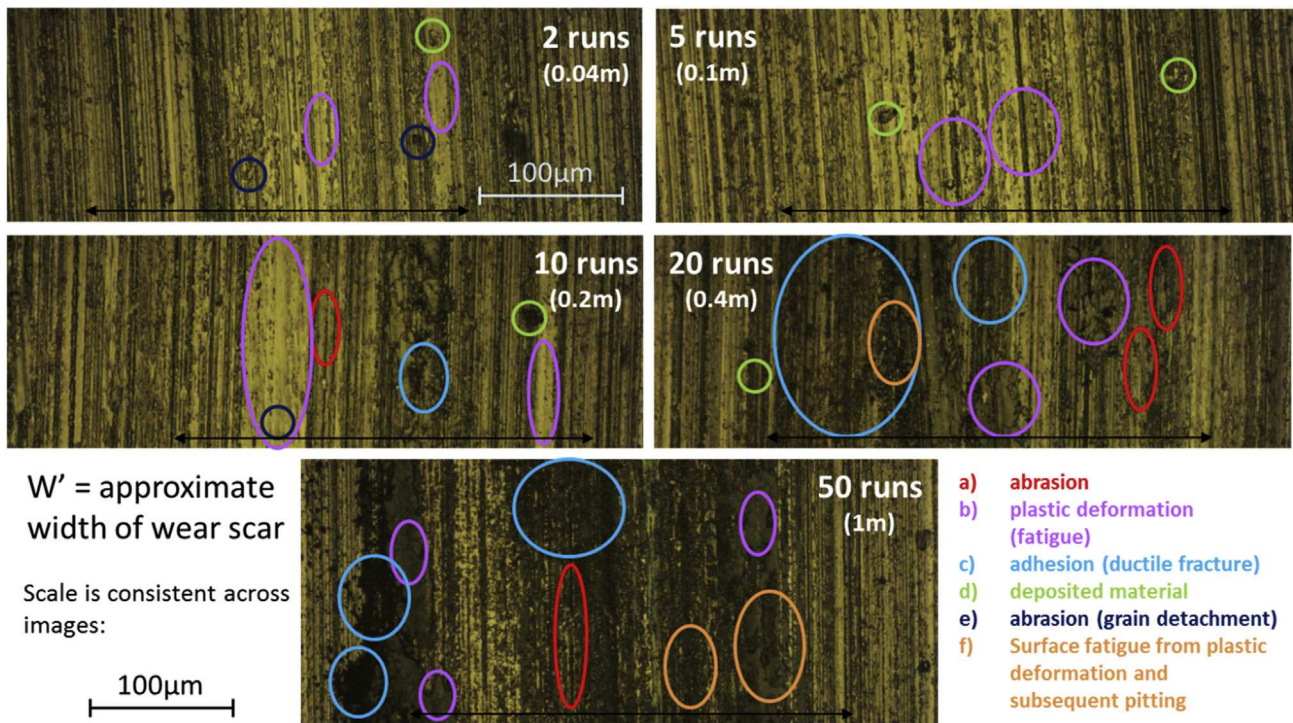The disparities in wear rates and failure mechanisms for micro and

Fig. 21. Wear of the TiB$_2$ coating is observed optically after 2, 5, 10, 20 and 50 runs.

macro tools are due to the geometrical properties of the tools and altered machining conditions, rather than then primary wear mechanisms. The addition on this scale of factors such as high machining stresses, impact due to interrupted cutting and small tool grains result in two outcomes:

(1) Increased significance of primary wear mechanisms (for example, material removal having relatively higher significance).

(2) Addition of volatile mechanical failure mechanisms such as chipping, cracking, and flaking of coatings.

As the process is scaled down, these mechanisms become more dominant and wear of tools becomes less predictable. Explanations for this include the mechanical stresses described due to tool geometries, and thermal cycling which is extreme due to the very small tool-workpiece interface area and the limitations of cooling systems at the
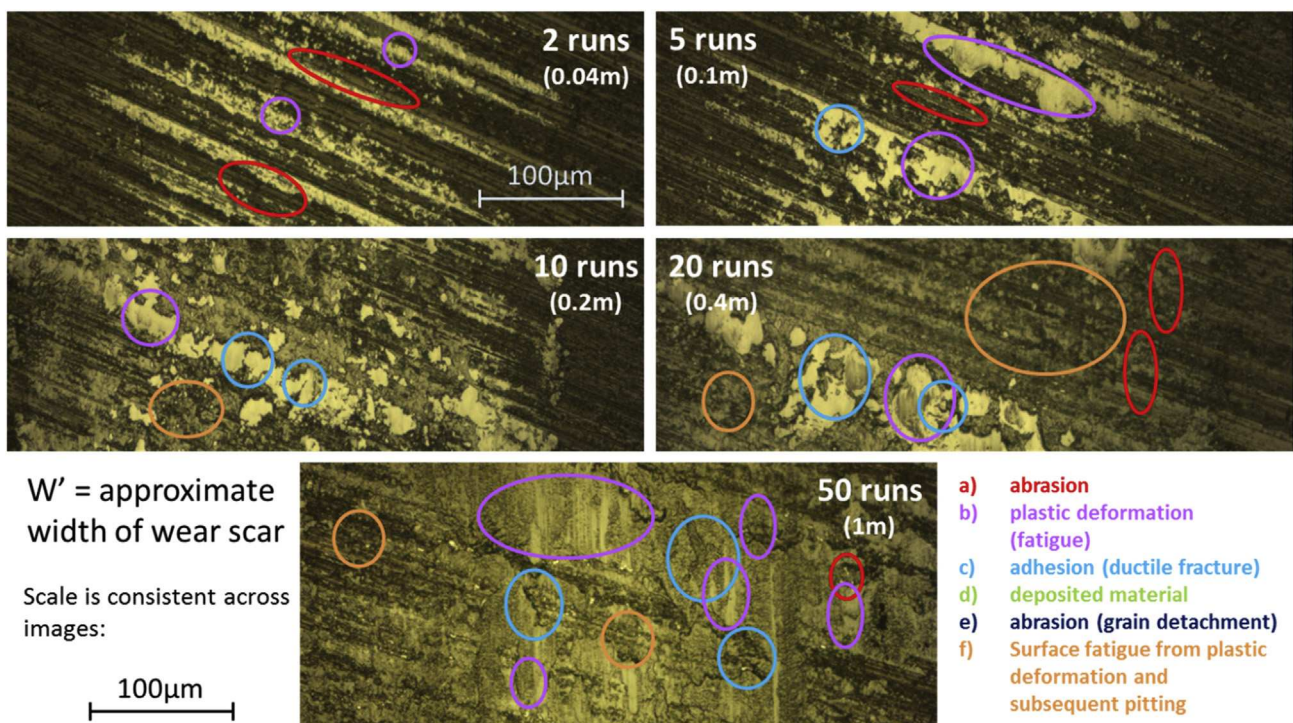

Fig. 22. Wear of the TiAlN/TiSiN coating is observed optically after 2, 5, 10, 20 and 50 runs.
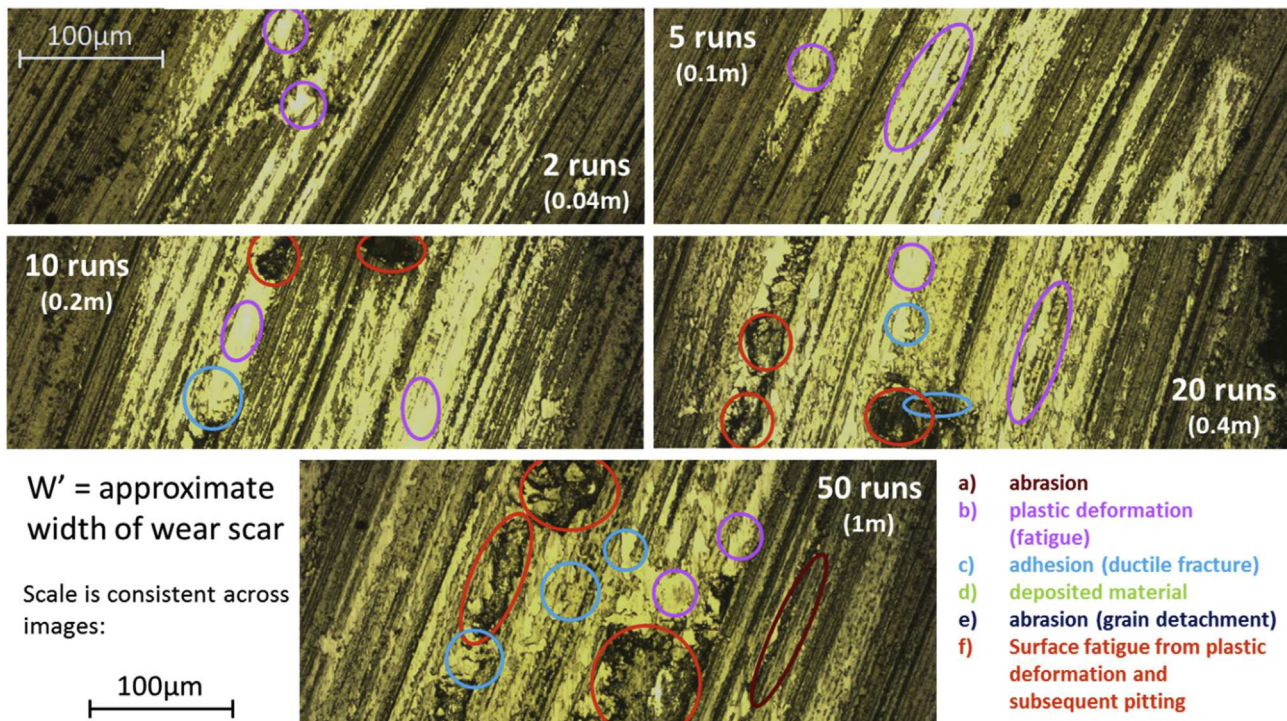
Fig. 23. Wear of the AlTiCrN coating is observed optically after 2, 5, 10, 20 and 50 runs.

smaller scale. The combination of thermal cycling and high mechanical stresses caused by tool geometries means that, relatively speaking, the types of wear that cause catastrophic failure such as chipping, attrition, and cracking occur more. Abrasion, which generally dominates the macro tool wear, has less of an effect.

4.6. Use of wear curves and pin-on disc as tools to evaluate coatings

Pin-on-disc represents a simple method of comparing some of the behaviours of different coatings seen, even in a micro-milling environment. Meanwhile, production of wear curves using situational testing allows a comparison between coatings in a real-life environment, and provides an insight into wear mechanisms seen, highlighting behavioural differences between micro and macro. However, direct testing of tools is time-consuming and expensive.

Results from both pin-on-disc testing and micromachining tests showed that for both brass and NiMo, it was possible to extend the SSR: RIP of the wear curves. In both cases SSR was proportionally longer for the coating which performed better. This extending of the steady state has two functions: first, it extends the overall life of the tool. Secondly, crucially, it extends the working life of the tool, during which wear can be predicted from the gradient found in stage II of wear. Simply extending overall length of tool life does not improve wear predictability and is thus not a useful result.

The method presented here of evaluating the effect coatings have on tool life is significantly more useful than simply comparing absolute wear of the tools since absolute wear does not necessarily indicate tool life.

5. Conclusions

Important results have been presented here that demonstrate a decrease in tool wear and thus improvements to machining accuracy and reduced production costs. In doing so, this work has considered the elongation of the SSR of the tool wear curve for micromilling as a means to improve the prediction of the evolution of tool wear. This allows cutting processes to be modified to maximise geometrical accuracy as

the tool wears and to measure the efficacy of applying different coatings to micro tools.

The following conclusions can be drawn:

(1) For each material investigated, one of the coatings yielded a longer SSR. It can therefore be concluded that coating design can be used to extend the length of the steady state wear region and not simply reduce overall tool wear.
(2) RIP:SSR ratio is a novel metric and associated methodology of assessing the performance of tools. The relatively shorter run-in periods for some coating/material combinations indicate that different coatings result in different RIP:SSR ratios. It is important that appropriate coatings are selected to reduce the length of tool run-in, thus allowing the SSR to be reached more quickly.
(3) Despite the difficulty measuring micro-tool wear and differences in wear mechanisms that dominate for macro-tools and micro-tools, it is possible to combine tool wear curves for micro-end-mills with pin-on-disc testing to evaluate coatings, highlighting similarities seen between micro and macro-tool wear. This can be harnessed when predicting tool wear.
(4) Observation of wear and COF using pin-on-disc tests, combined with wear observed in a machining scenario, allows the differences in wear at the macro and micro-scale to be better understood: the small sizes of micro-milling tools, small cutting-edge radius, corresponding high temperatures and stresses result in additional wear mechanisms that are seen less on the macro scale.
(5) While abrasive and adhesive mechanisms dominate in macro-milling, at the micro-scale the effects of impact wear and cracking are exacerbated due to relatively large workpiece grain size and very high stresses where tool-workpiece contact is small.
(6) There is value in further investigating both the novel application of coatings that have previously only be used in a macro-milling and in modifying the design of these coatings to increase the SSR of the tools.

Acknowledgements

The authors wish to acknowledge the contribution of D.T. Curtis of the University of Sheffield Advanced Manufacturing Research Centre to discussions regarding tool wear; the contribution of tools from Kyocera-SGS; and the financial support of the EPSRC EP/I01800X/1 in this work.

Appendix A. Supplementary data

Supplementary data to this article can be found online at https://doi.org/10.1016/j.precisioneng.2019.07.018.

References

[1] Jemielniak K, Arrazola PJ. Application of AE and cutting force signals in tool condition monitoring in micro-milling. CIRP J. Manuf. Sci. Technol. 2008;1(2):97–102.
[2] Astakhov VP. Tribology of metal cutting vol. 52. Elsevier; 2006.
[3] Groover MP. Groover's principles of modern manufacturing: materials, processes, and systems. Wiley; 2016.
[4] Shao H, Liu L, Qu HL. Machinability study on 3% Co–12% Cr stainless steel in milling. Wear 2007;263(1–6):736–44.
[5] Tansel I, Rodriguez O, Trujillo M, Paz E, Li W. Micro-end-milling - I. Wear and breakage. Int J Mach Tool Manuf 1998;38(12):1419–36.
[6] Chae J, Park SS, Freiheit T. Investigation of micro-cutting operations. Int J Mach Tool Manuf 2006;46(3):313–32.
[7] Mian AJ, Driver N, Mativenga PT. Identification of factors that dominate size effect in micro-machining. Int J Mach Tool Manuf 2011;51(5):383–94.
[8] Liu X, DeVor RE, Kapoor SG, Ehmann KF. The mechanics of machining at the microscale: assessment of the current state of the science. J Manuf Sci Eng 2004;126(4):666–78.
[9] Camara MA, Rubio JCC, Abrão AM, Davim JP. State of the art on micromilling of materials, a review. J Mater Sci Technol 2012;28(8):673–85.
[10] Lai X, Li H, Li C, Lin Z, Ni J. Modelling and analysis of micro scale milling considering size effect, micro cutter edge radius and minimum chip thickness. Int J Mach Tool Manuf 2008;48(1):1–14.
[11] Saedon JB, Soo SL, Aspinwall DK, Barnacle A, Saad NH. Prediction and optimization of tool life in micromilling AISI D2 (~ 62 HRC) hardened steel. Procedia Eng. 2012;41:1674–83.
[12] Sarhan A, Sayed R, Nassr AA, El-Zahry RM. Interrelationships between cutting force variation and tool wear in end-milling. J Mater Process Technol 2001;109(3):229–35.
[13] Wang Y, Zou B, Huang C, Liu Z, Yao P. The micro-cutting performance of cermet and coated WC micro-mills in machining of TC4 alloy micro-grooves. Int J Adv Manuf Technol 2018;96:1–4.
[14] Baharudin BTHT, Dimou N, Hon KKB. Tool wear behaviour of micro-tools in high speed CNC machining. In proceedings of the 34th international MATADOR conference. 2004. p. 111–8.
[15] Teng X, Huo D, Shyha I, Chen W, Wong E. An experimental study on tool wear behaviour in micro milling of nano Mg/Ti metal matrix composites. Int J Adv Manuf Technol 2018;96:5–8.
[16] Rajabi A, Ghazali MJ, Syarif J, Daud AR. Development and application of tool wear: a review of the characterization of TiC-based cermets with different binders. Chem Eng J 2014;255:445–52.
[17] Oliaei SNB, Karpat Y. Influence of tool wear on machining forces and tool deflections during micro milling. Int J Adv Manuf Technol 2016;84(9–12):1963–80.
[18] Filiz S, Conley CM, Wasserman MB, Ozdoganlar OB. An experimental investigation of micro-machinability of copper 101 using tungsten carbide micro-endmills. Int J Mach Tool Manuf 2007;47(7):1088–100.
[19] Alhadeff LL, Marshall MB, Curtis DT, Slatter T. Protocol for tool wear measurement in micro-milling. Wear 2019;420–421.
[20] Aramcharoen A, Mativenga PT, Yang S, Cooke KE, Teer DG. Evaluation and selection of hard coatings for micro milling of hardened tool steel. Int J Mach Tool Manuf 2008;48(14):1578–84.
[21] Irfan Ucun, Aslantas K, Bedir F. An experimental investigation of the effect of coating material on tool wear in micro milling of Inconel 718 super alloy. Wear 2013;300(1–2):8–19.
[22] Lahres M, Müller-Hummel P, Doerfel O. Applicability of different hard coatings in dry milling aluminium alloys. Surf Coat Technol 1997;91(1–2):116–21.
[23] Bian R, He N, Ding W, Liu S. A study on the tool wear of PCD micro end mills in ductile milling of ZrO 2 ceramics. Int J Adv Manuf Technol 2017;92(5–8):2197–206.
[24] Dweiri F, Al-Jarrah M, Al-Wedyan H. Fuzzy surface roughness modeling of CNC down milling of Alumic-79. J Mater Process Technol 2003;133(3):266–75.
[25] Lekkala R, Bajpai V, Singh RK, Joshi SS. Characterization and modeling of burr formation in micro-end milling. Precis Eng 2011;35(4):625–37.
[26] Lin Y-J, Agrawal A, Fang Y. Wear progressions and tool life enhancement with AlCrN coated inserts in high-speed dry and wet steel lathing. Wear 2008;264(3–4):226–34.
[27] Zareena AR, Veldhuis SC. Tool wear mechanisms and tool life enhancement in ultra-precision machining of titanium. J Mater Process Technol 2012;212(3):560–70.
[28] Neves D, Diniz AE, Lima MSF. Microstructural analyses and wear behavior of the cemented carbide tools after laser surface treatment and PVD coating. Appl Surf Sci 2013;282:680–8.
[29] Biermann D, Steiner M, Krebs E. Investigation of different hard coatings for micromilling of austenitic stainless steel. Procedia CIRP 2013;7:246–51.
[30] Ezugwu EO, Wang ZM. Titanium alloys and their machinability - a review. J Mater Process Technol 1997;68(3):262–74.
[31] Prengel HG, Pfouts WR, Santhanam AT. State of the art in hard coatings for carbide cutting tools. Surf Coat Technol 1998;102(3):183–90.
[32] Fox-Rabinovich GS, et al. Design and performance of AlTiN and TiAlCrN PVD coatings for machining of hard to cut materials. Surf. coatings Technol. 2009;204(4):489–96.
[33] Faga MG, et al. AlSiTiN nanocomposite coatings developed via Arc Cathodic PVD: evaluation of wear resistance via tribological analysis and high speed machining operations. Wear 2007;263(7–12):1306–14.
[34] Sui X, et al. Relationship of microstructure, mechanical properties and titanium cutting performance of TiAlN/TiAlSiN composite coated tool. Ceram Int 2016;42(6):7524–32.
[35] Dobrzański LA, Pakuła D. Comparison of the structure and properties of the PVD and CVD coatings deposited on nitride tool ceramics. J Mater Process Technol 2005;164:832–42.
[36] Hedenqvist P, Olsson M. Sliding wear testing of coated cutting tool materials. Tribol Int 1991;24(3):143–50.
[37] Jianxin D, Jianhua L, Jinlong Z, Wenlong S, Ming N. Friction and wear behaviors of the PVD ZrN coated carbide in sliding wear tests and in machining processes. Wear 2008;264(3–4):298–307.
[38] Aihua L, Jianxin D, Haibing C, Yangyang C, Jun Z. Friction and wear properties of TiN, TiAlN, AlTiN and CrAlN PVD nitride coatings. Int J Refract Metals Hard Mater 2012;31:82–8.
[39] Reymondin C-A. *The theory of horology*. Swiss federation of technical colleges [and] the watchmakers of Switzerland training and educational program Neuchaˆtel in collaboration with GREME. 1999.
[40] Elias CN, Lima JHC, Valiev R, Meyers MA. Biomedical applications of titanium and its alloys. JOM (J Occup Med) 2008;60(3):46–9.
[41] Davis JR. Handbook of materials for medical devices. ASM international; 2006.
[42] Chen Q, Thouas GA. Metallic implant biomaterials. Mater Sci Eng R Rep 2015;87:1–57.
[43] Zhu D, Zhang X, Ding H. Tool wear characteristics in machining of nickel-based superalloys. Int J Mach Tool Manuf 2013;64:60–77.
[44] Nobel C, Klocke F, Lung D, Wolf S. Machinability enhancement of lead-free brass alloys. Procedia CIRP 2014;14:95–100.
[45] Corduan N, et al. Wear mechanisms of new tool materials for Ti-6AI-4V high performance machining. CIRP Ann. 2003;52(1):73–6.
[46] Cheng X, Wang Z, Nakamoto K, Yamazaki K. A study on the micro tooling for micro/nano milling. Int J Adv Manuf Technol 2011;53(5–8):523–33.
[47] Nouari M, Makich H. On the physics of machining titanium alloys: interactions between cutting parameters, microstructure and tool wear. Metals (Basel). 2014;4(3):335–58.
[48] Ginting A, Nouari M. Surface integrity of dry machined titanium alloys. Int J Mach Tool Manuf 2009;49(3–4):325–32.
[49] Dehlinger A-S, et al. Influence of Cr and Si addition on structural and mechanical properties of TiAlN coatings reactively sputter deposited. Plasma Process Polym 2007;4(S1):S588–92.
[50] Feng C, et al. Effects of Si content on microstructure and mechanical properties of TiAlN/Si3N4-Cu nanocomposite coatings. Appl Surf Sci 2014;320:689–98.
[51] Paiva JM, et al. Tribological and wear performance of carbide tools with TiB2 PVD coating under varying machining conditions of TiAl6V4 aerospace alloy. Coatings 2017;7(11):187.